Supplementary Materials for

A Reversible Plasmonic Nanoprobe for Dynamic Imaging of Intracellular pH during Endocytosis

Jin Wang[1], Qiao Yu[1], Xiang-Ling Li[2]*, Xueli Zhao[3], Hong-Yuan Chen[1], Jing-Juan Xu[1]*

[1] State Key Laboratory of Analytical Chemistry for Life Science, School of Chemistry and Chemical Engineering, Nanjing University, Nanjing 210023, P.R. China.
[2] College of Life Science and Pharmaceutical Engineering, Nanjing Tech University, Nanjing 211816, P.R. China.
[3] College of Chemistry and Molecular Engineering, Zhengzhou University, Zhengzhou 450001, China
*Corresponding author: Tel/ fax: +86-25-89687924, Email: xujj@nju.edu.cn (J.-J. Xu), xlli@njtech.edu.cn. (X.-L. Li)

Contents

1. Reagents and apparatus

Chemicals and Materials. Hydrochloric acid (HCl) and ethanol were purchased from Sinopharm Chemical Reagent Co., Ltd.. Sodium dodecyl sulfate (SDS), aniline, and ammonium persulfate were obtained from Aladdin. Nigericin and dimethyl sulfoxide were purchased from Sigma-Aldrich. Phosphate-buffered solution (PBS, 10 mM, pH ~7.3), and Dulbecco's modified Eagle's medium (DMEM) were obtained from Keygen Biotechnology Co., Ltd. (Nanjing, China). CellLight Early Endosomes-GFP, BacMam 2.0 and CellLight Late Endosomes-GFP, BacMam 2.0 ware obtained from Thermo Fisher Technology (China) Co., Ltd.. Lyso-Tracker Green was bought from Beyotime Biotechnology. Deionized water was used throughout the process.

Apparatus. High-resolution transmission electron microscopy (TEM) was performed with a JEM-2100 transmission electron microscope (JEOL Ltd., Japan). UV-*vis* extinction spectra were recorded on a UV-*vis* spectrophotometer (Nanodrop-2000C, Nanodrop, USA). The ζ-potential was acquired with a Malvern instrument (Nano-Z, Malvern Instruments Ltd., Britain). The dark-field measurements were carried out on an inverted microscope (IX71, Olympus) that was equipped with a dark-field condenser ($0.8 < NA < 0.92$) and a 60× objective lens (NA = 0.7). A 100 W halogen lamp was used as the white light source. A true-color digital camera (Olympus DP80, Japan) was used to capture the dark-field color images and fluorescence images. The scattering light of the nanoparticle was split by a monochromator (Acton SP2358, PI, USA) equipped with a grating (grating density, 300 lines/mm; blazed wavelength, 500 nm). In all of the dark-field imaging experiments in this paper, the experimental conditions were consistent with a light intensity of 50% and an exposure time of 300 ms.

2. Characterization of the AuNPs and Au@PANI NPs

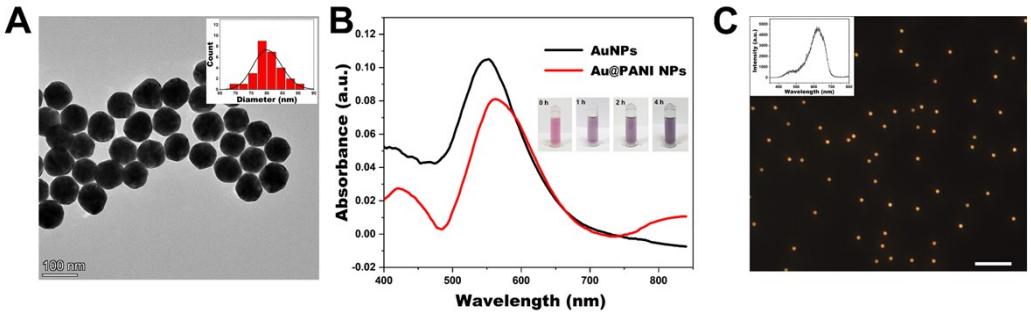

Figure S1 (A) TEM image of the synthesized 80 nm AuNPs. Insert: size distribution of 80 nm-AuNPs. (B) UV-*vis* spectra of 80 nm AuNPs and Au@PANI NPs in pH 7.3 PBS. Insert: color changes over time during the Au@PANI NPs synthesis process. (C) Representative DFM images of Au@PANI NPs in PBS (pH 7.3). Insert: Typical Scattering spectrum of Au@PANI at pH 7.3 in PBS. Scale bar: 5 μm.

3. The feasibility of the Au@PANI NPs response to pH changes

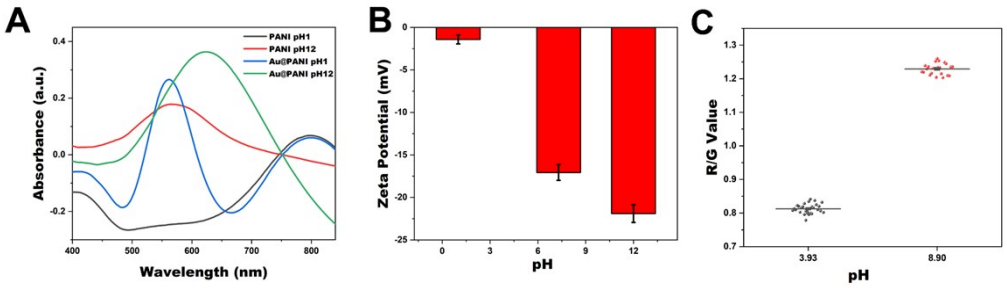

Figure S2 (A) The UV-*vis* spectra of PANI and Au@PANI at pH 1 and pH 12, respectively. It indicated that the absorbance peak of ~ 800 nm at pH 1 of Au@PANI belonged to the PANI. (B) Zeta potential variation of Au@PANI dispersed in PBS of pH 1, pH 7.4, and pH 12 conditions. (C) The R/G value statistics of Au@PANI NPs in PBS with different pH (pH 3.93 and pH 8.90)

4. The pH-responsive properties of the scattering signal of Au@PANI NPs

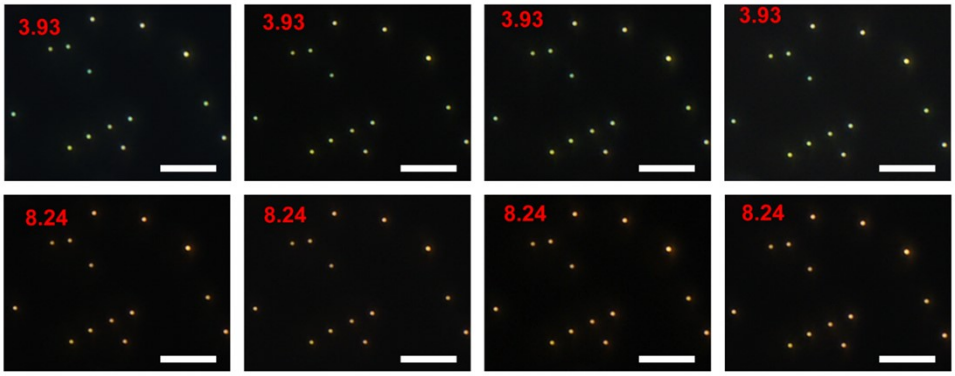

Figure S3 (A) DFM images of Au@PANI NPs during four cycles at pH 3.93 and 8.24 alternatively. Scale bar: 5 μm.

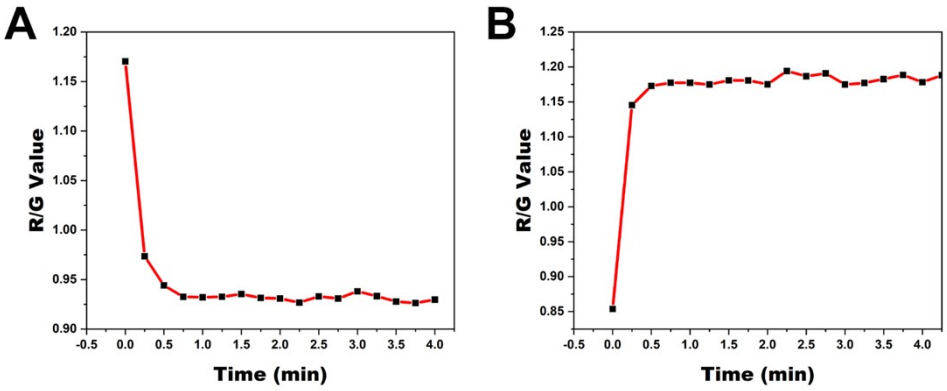

Figure S4 The scattering signal evolution of Au@PANI with time when changed the pH from 8.24 to 3.93 (A) and 3,93 to 8.24 (B).

5. Quantitative detection of pH *via* Au@PANI nanoprobes

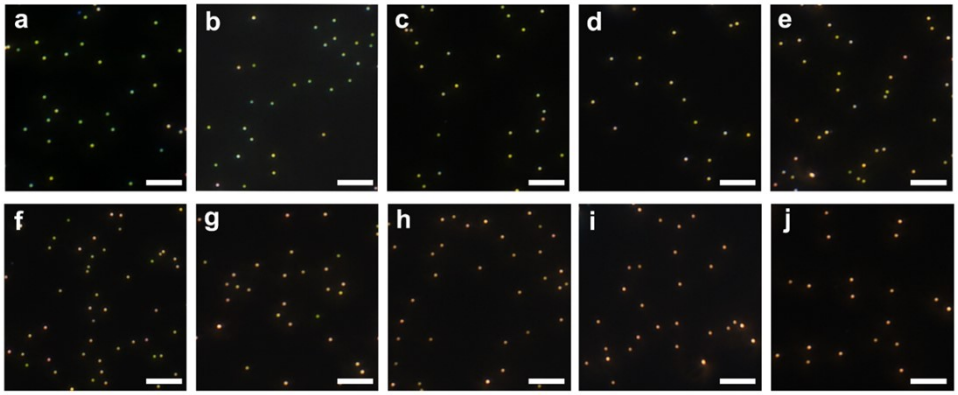

Figure S5 DFM images of the Au@PANI nanoprobes in PBS with different pH values (a-j: 3.93, 4.31, 4.86, 5.39, 5.89, 6.3, 6.84, 7.35, 7.73, and 8.24). Scale bar, 5 μm.

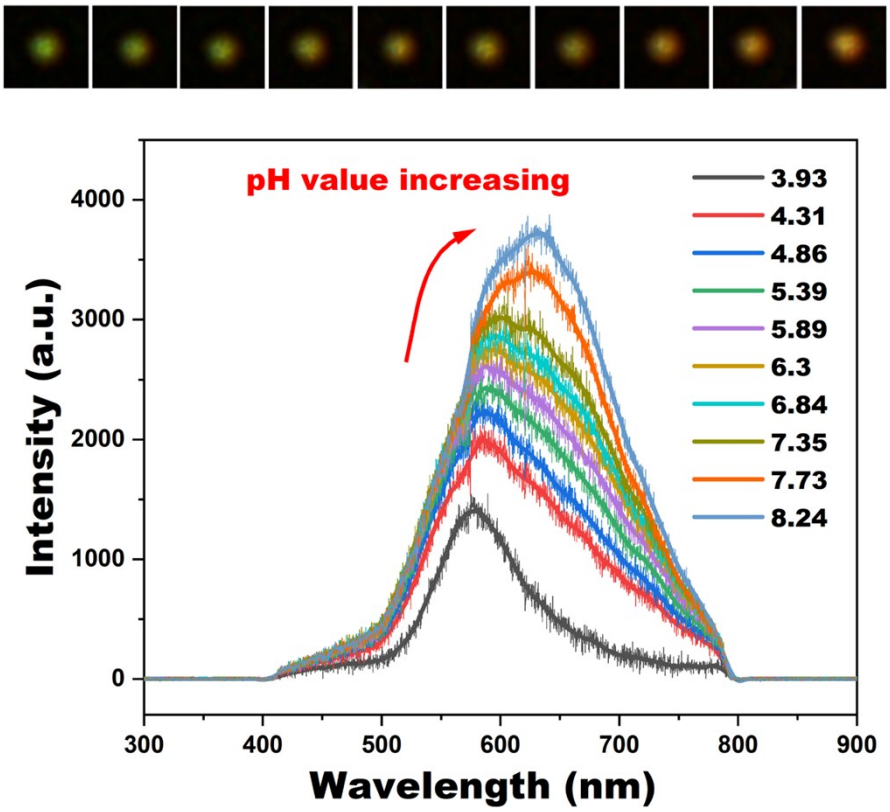

Figure S6 DFM images and the scattering spectra of single Au@PANI nanoprobe. It revealed that the nanoparticles gradually changed from green to orange-red with increasing pH, while the single-particle scattering spectra also exhibited a gradual redshift accompanied by an increase in the scattering intensity.

6. The selectivity of Au@PANI NPs towards pH and the stability

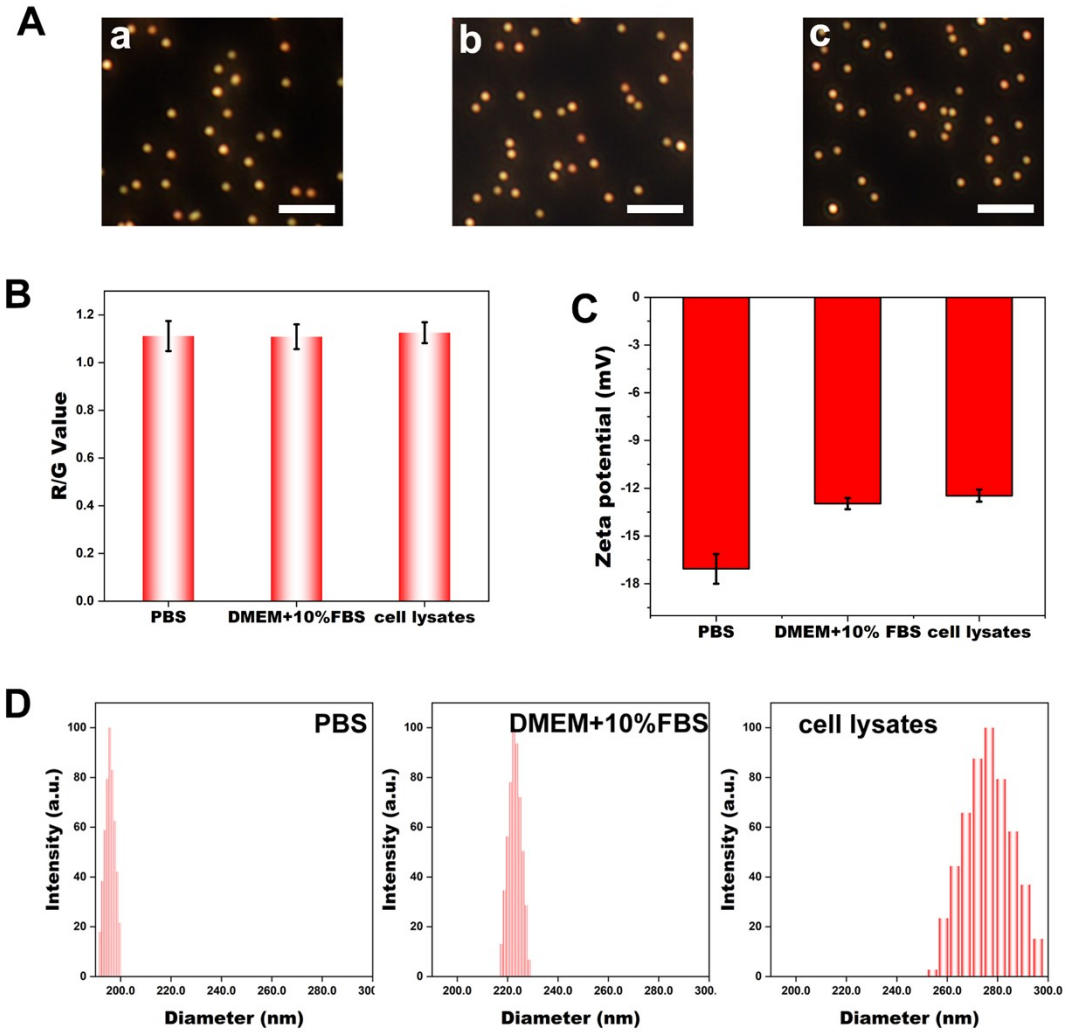

Figure S7 Stability assessment of nanoprobes**.** (A) DFM images of Au@PANI NPs after dispersed in PBS, DMEM + 10% FBS, and cell lysates for 24 h, respectively. Scale bar: 2 μm. (B) The statistics of R/G values of Au@PANI NPs in (A). (C-D) The zeta potential (C) and DLS (D) variation of Au@PANI NPs dispersed in different solutions for 24 h. The results revealed that the negative potential of Au@PANI NPs became smaller and the DLS increased in cell culture medium and cell lysate, which may be caused by the adsorption of peptides or protein macromolecules.

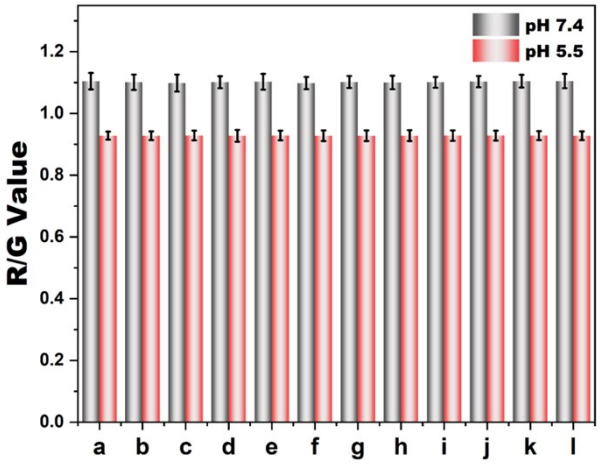

Figure S8 (A) The R/G value of Au@PANI NPs after adding different potential interferences (a-l: K^+, Mg^{2+}, Na^+, Ca^{2+}, Cl^-, SO_4^{2-}, CO_3^{2-}, glutathione, glucose, cysteine, and H_2O_2. The concentration of all substances is 100 mM). The effects of different potential interferences are examined in PBS buffer with pH values of 7.4 or 5.5. Error bars indicate the standard deviation of 30 nanoparticles.

7. Cytotoxicity study on Au@PANI nanoprobes

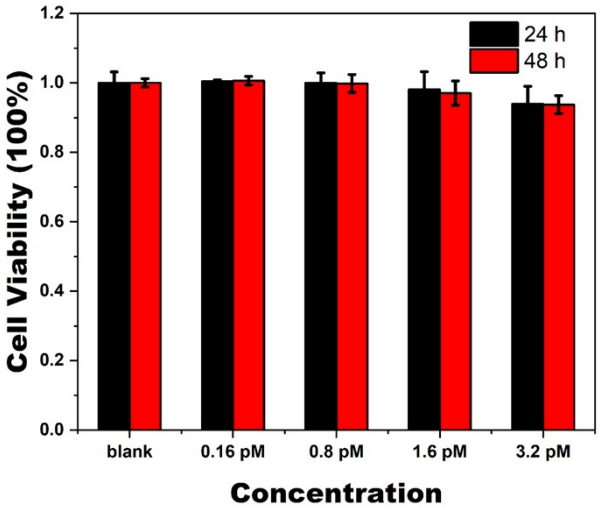

Figure S9 (A) The cell viability after being incubated with different concentrations of Au@PANI NPs for 24 h or 48 h. The results indicated that the Au@PANI NPs possessed excellent biocompatibility and still keep the viability near 100% after being incubated with 1.6 pM Au@PANI NPs for 48 h.

8. Investigation of the endocytosis mechanism of Au@PANI NPs

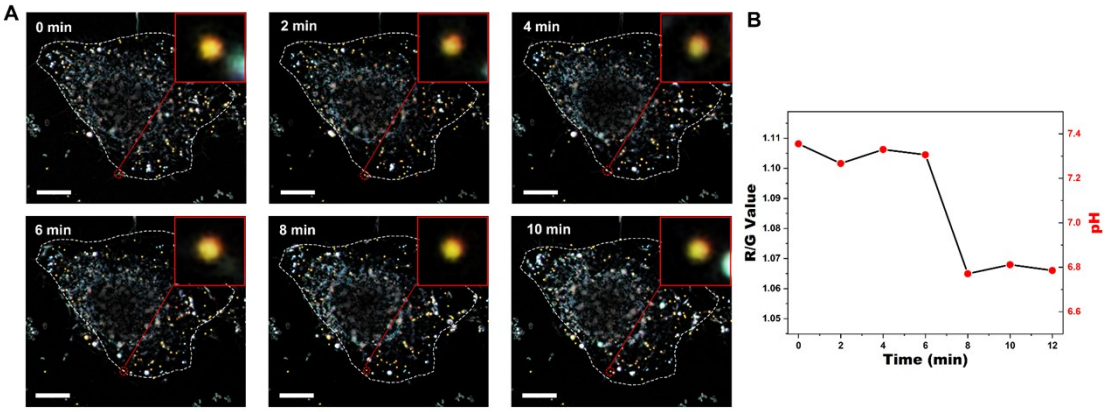

Figure S10 The endocytosis process of Au@PANI nanoprobes. (A) Time-dependent DFM images of HeLa cells during the endocytosis process. Scale bar: 10 μm. (B) The plot of R/G value changes of the nanoprobe circled in (A) *versus* time.

After incubating the probes with cells for 1 h, a fresh culture medium was added, and then the nanoparticles adjacent to the cell membrane but not endocytosed were selected for real-time tracking by dark-field imaging. As seen in Figure S10, the nanoprobe gradually approached the cell membrane with time. The scattering signal fluctuated slightly during the first 6 min, with the pH value maintained around 7.3, which was exactly the pH range of the cell culture medium. After 6 min, we observed that the probe had completely entered the cell, with the R/G value suddenly decreased and the pH started to be maintained around 6.8, indicating that the probe was endocytosed from extracellular to intracellular.

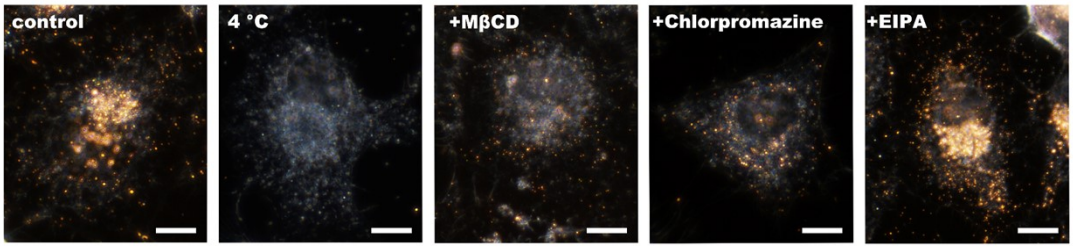

Figure S11 DFM images of cellular uptake of Au@PANI NPs after cells were treated with different endocytosis inhibitors. Scale bar: 10 μm.

9. Statistical results of co-localization experiments

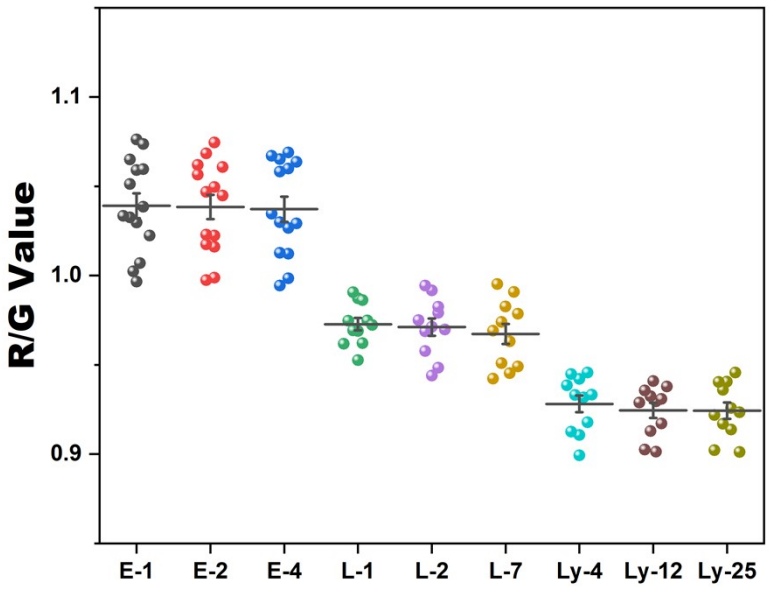

Figure S12 The R/G value distribution over time for early, late endosomes and lysosomes, respectively.

10. TEM images of HeLa cells treated with Au@PANI NPs

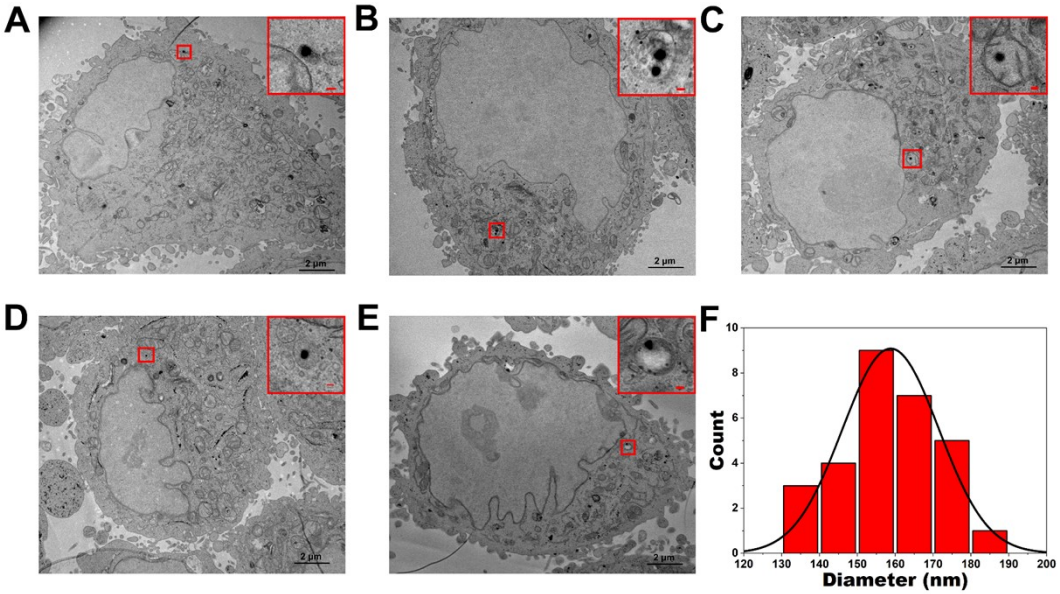

Figure S13 (A-E) Representative TEM images for the time evolution of Au@PANI NPs incubated with HeLa cells for 0 h (A), 1 h (B), 2 h (C), 4 h (D), and 6 h (E). Scale bar: 2 μm (insert: 100 nm). (F) The diameter distribution of the endocytosed Au@PANI NPs.

11. Detecting the pH evolution during endosomal maturation process in living cells

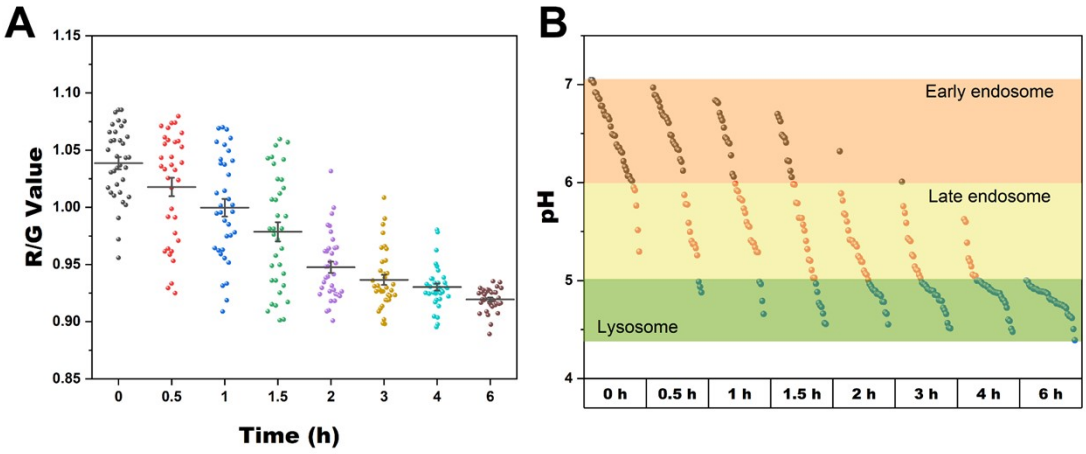

Figure S14 (A) Statistical analysis of R/G value distributions of Au@PANI NPs in HeLa cells after further incubation for different times. HeLa cells were treated with 0.16 pM Au@PANI NPs for 1 h in advance followed by washing with PBS and further incubating in complete DMEM for different times. (B) The calculated pH distribution for selected time points throughout the experiment. Highlighted boxes represented typical pH values of early endosome (orange, pH 7.0-6.0), late endosome (yellow, pH 6.0-5.0), and lysosome (green, pH 5.0-4.4)